ALTERNATIVE MEASURE FOR PERFORMANCE OF HLW GEOLOGIC REPOSITORY

Joonhong Ahn and Paul L. Chambré
Department of Nuclear Engineering
University of California, Berkeley
Berkeley, California 94720-1730
USA

ABSTRACT

A repository performance model that can show effects of canister multiplicity and repository configuration has been developed. Masses of a radionuclide in the repository and in the far field are proposed as performance measures. Canister multiplicity has significant effects on the release of long-lived radionuclides from the repository. As more canisters are included in the same water stream, the radionuclide concentration in the stream increases, but becomes independent of the number of canisters for sufficiently many canisters. Effects of reduction of radionuclide mass in the repository on the repository performance are clearly observed if the canister multiplicity is taken into account and the mass-based measures are applied.
Keywords: Repository performance measures, Canister multiplicity, Radionuclide mass, Partitioning and Transmutation

1- INTRODUCTION

The effects of nuclear-fuel cycle schemes manifest themselves by differences in masses of radionuclides contained in the waste. However, previous analyses [1,2] of the impacts of Partitioning-and-Transmutation (P-T) systems on the performance of geologic disposal conclude that P-T systems are not justified due to their high costs and modest improvements in radiological safety. This conclusion is primarily based on the observation that, due to low solubilities of actinides in groundwater, a decrease in the masses of actinides in the waste does not decrease the radiological impact of actinides in a proportional manner [2,3,4].

In previous performance assessments for a high-level radioactive waste (HLW) repository, the mass of radionuclide released from a single waste canister per unit time (independent of other canisters) is first obtained, and then used as the inlet boundary condition for the radionuclide transport into the far-field region. The repository is regarded as a collection of such independent single canisters.

An actual repository, however, consists of thousands of waste canisters. There can be important effects of the number of canisters and interaction among multiple waste canisters on the release of radionuclides from the repository. It is likely that predicted repository performance is insensitive to fuel cycle schemes because

- Repository performance is currently measured by exposure dose rates determined by concentrations of radionuclides in groundwater in the far field, and
- In previous performance assessments, models of radionuclide transport in sub-regions, such as the engineered barriers, near-field rock, and far-field rock, have been inadequately combined together into a total performance model, so that radionuclide concentrations in groundwater in the far field may not be properly evaluated.

In the present study, a new repository performance model is established, where the radionuclide concentration in the water leaving the repository is obtained by taking into account the effects of interaction among multiple canisters. To illustrate, we consider transport of ^{237}Np in two different configurations. In configuration (1), N canisters are lined up in the direction parallel to the water flow in the near field rock. In configuration (2), which is the one applied in previous assessment studies, N canisters are lined up in the direction perpendicular to the water flow. In this configuration, all canisters are assumed to act independently with each other.

Mass balance equations for the single radionuclide in the waste matrix, in the Engineered-Barrier System (EBS), and in the near-field rock (NFR) are established by considering solubility-limited release from the waste matrix to the EBS. Radionuclide diffusion in the EBS, coupled with advective transport in the NFR, and linear sorption isotherm between the solid phase and the water phase in the EBS and in the NFR are taken into account. From the downstream end of a row of canisters, the radionuclide is released into the far field. A separate balance equation has been written for the mass of the radionuclide in the far field.

With the model, the masses of the radionuclide in the repository region and in the far-field region are obtained as well as the radionuclide concentration in the water leaving the repository. Repository performance measures based on radionuclide masses could sensitively reflect differences in fuel cycle schemes. Such measures are useful for comparing one nuclear-fuel-cycle scheme with another from the viewpoint of repository performance.

2- PREVIOUS PERFORMANCE ASSESSMENT MODELS

Previous performance-assessment models were developed for single-canister configuration [3,5,6,7] (See Figure 1). The EBS analysis determines the mass release rate, Q, of a radionuclide from the EBS into the

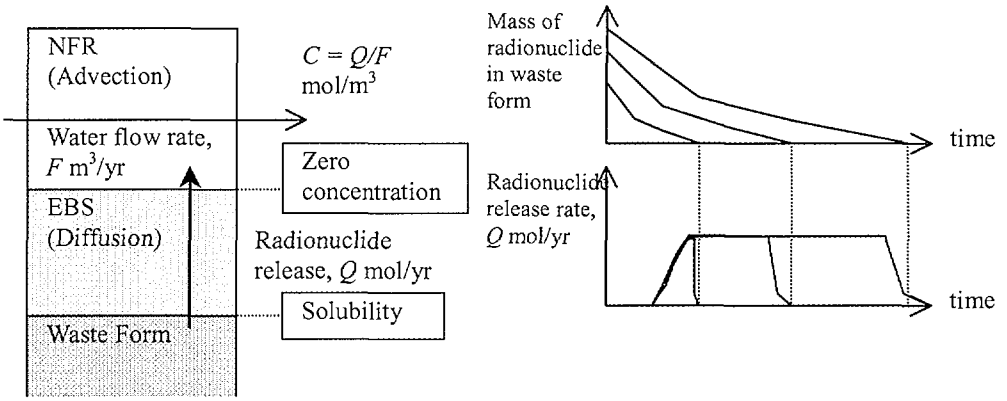

Figure 1: Previous performance assessment model with a single-canister configuration. (In the left figure, the EBS region is considered to be diffusion-dominated. The radionuclide concentration at the EBS-waste form interface is constant at the solubility. The concentration is assumed to be zero at the EBS-NFR interface. On the right, three curves depict effects of reduction in the radionuclide mass in the waste form. Due to the solubility limit at the waste form surface, the magnitude of the release rate, Q, does not change by reduction of radionuclide mass, whereas the duration of the release is reduced. The concentration, C, in water leaving is determined by assuming an arbitrary water flow rate, F.)

surrounding NFR. The mass of the radionuclide in the waste form decreases with time due to its decay and the release into the EBS. In the EBS, molecular diffusion is considered to be dominant. For actinide elements with limited solubilities, the concentration at the waste-form surface in water is limited by the elemental solubility. At the outer boundary of the EBS, i.e., at the interface between the EBS and NFR, the radionuclide concentration is often assumed to be zero [3,5,6,7], in order to decouple the transport problem inside the EBS from that in the exterior region. For a long-lived actinide such as ^{237}Np, the concentration profile in the EBS reaches a steady state, ranging between the solubility at the inner boundary and the zero concentration at the outer boundary.

For the far-field transport analysis, the inlet boundary concentration, C, is determined by

$$C = Q/F\,, \tag{1}$$

by assuming an arbitrary water flow rate, F, in the surrounding NFR. With this concentration, C, as the inlet boundary condition, the concentration, C', of the radionuclide at a certain point downstream from the repository in the far field is evaluated by the far-field transport analysis. A transport analysis in the biosphere, then, utilizes the concentration, C', and gives a value of the performance measure such as the exposure dose rate (Sv/yr). Thus, the radionuclide concentration, C, determines the magnitude of the performance measure.

By decreasing the mass of the radionuclide in the waste form, the duration of the radionuclide release into the surrounding NFR is reduced, but not the magnitude of the release rate, Q (see the right figure of Figure 1). This is because the release of the radionuclide from the waste form is limited by the solubility in groundwater. The decrease in the radionuclide mass does not affect the concentration, C, unless the mass reduction is so significant that the release is not limited by the solubility.

Consider that there are multiple identical canisters in the repository with identical EBS. We can consider two extreme configurations to take into account the canister multiplicity. In configuration (1), N canisters are lined up in the direction *parallel* to, and included in, the water flow in the NFR. In configuration (2), N canisters are lined up in the direction *perpendicular* to the water flow. In this configuration, all canisters are independent with each other. In previous performance assessments [3,5,7], the second configuration was assumed. In this configuration, the radionuclide concentration in the water entering the far field is equal to C for any number of

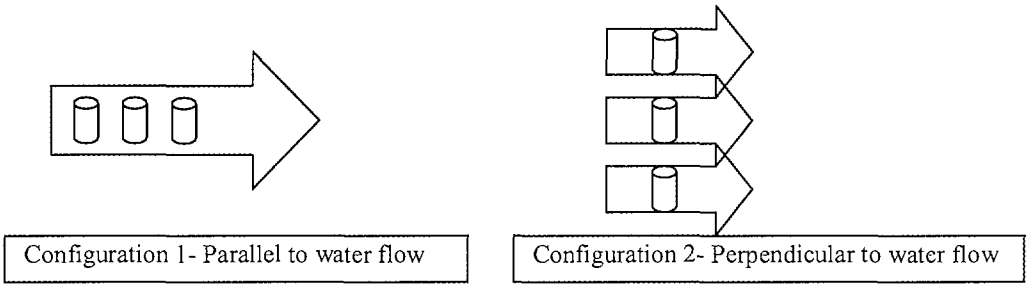

Figure 2: Canister configurations to water flow. Arrows represent water flow stream, to which radionuclides are released from canisters. Cylinders represent waste canisters.

canisters.

Therefore, if the inlet boundary concentration, C, is determined as mentioned above, and Configuration (2) is assumed, *no* effects on the exposure dose rates would be observed by reducing the mass of radionuclide in individual canisters or by reducing the number of canisters. We consider that this is the reason for the insensitivity observed in the previous studies for P-T effects on repository performance [1,3,8].

Suppose that we use the same single-canister model (Figure 1) with configuration (1) instead of (2). The radionuclide concentration in the NFR increases proportionally as the number of canisters included in the same water stream increases, because the identical release, Q, is added to the water stream by each waste canister. Canister configuration could actually affect the radionuclide concentration in water leaving the repository, and thus the exposure dose rate. But, previous performance assessment models did not take into account canister multiplicity. Hence, neglecting canister multiplicity could lead to underestimating the exposure dose rate.

The concentration of the radionuclide in water leaving after sweeping multiple canisters can increase indefinitely as the number of canisters included in the water stream increases. However, the concentration cannot exceed the solubility. This caveat results from the assumption that the concentration at the interface between the EBS and the NFR is equal to zero for decoupling the transport in the EBS from that in the NFR.

In the present model, canister multiplicity and the repository configuration are properly incorporated. Because effects of P-T schemes manifest themselves by reductions in masses of radionuclides contained in the waste, the repository performance should also be measured by masses of radionuclides. Numerical examples are shown to illustrate the effects of canister multiplicity (Section 4.1) and reduction of nuclide mass in individual canisters (Section 4.2).

3- MODEL

In the analysis, radionuclide transport in a hypothetical repository is modeled by considering a chain of compartments each containing a waste matrix, a buffer, and a NFR region (Figure 3). The EBS corresponds to the combined regions of the waste matrix and the buffer. A repository region is considered to consist of compartments connected by advective transport in the NFR regions. Canisters each containing a waste matrix are placed in a two dimensional array fashion. A row of N compartments in the repository is considered to be included in the same water stream. The region interior to all parallel compartments is called the repository region. The region exterior to the repository region is called the far-field region. The waste matrix is transformed into slab geometry with the same interfacial area, S [m^2], of the original cylindrical geometry.

The configuration shown in Figure 3 is schematically the same as Configuration (1) in Figure 2. Configuration (2) can be obtained by setting N equal to unity in Figure 3.

Radionuclide in the waste matrix is first transported by molecular diffusion through the buffer, and then by advection through the NFR. It is assumed that the water flow direction in the NFR is parallel to a row of compartments. By assuming that radionuclide transport is identical in two adjacent compartment-rows, it is also assumed that there is no net mass transport through the interface between the two rows. Hence, radionuclide transport in a single row of N compartments is considered in this study. Linear sorption isotherm between the solid phase and the pore water phase in the buffer and in the NFR is also assumed. Existence of precursors of a radionuclide and other isotopes of the element is neglected.

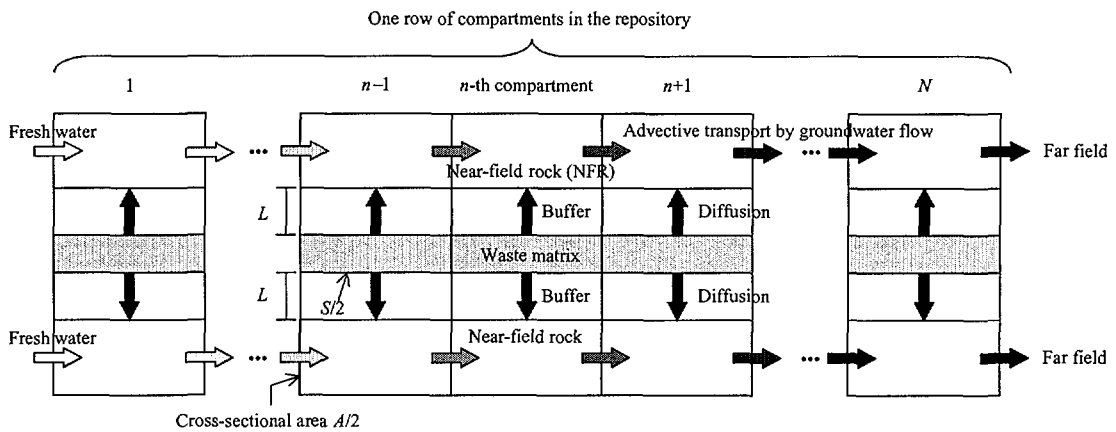

Figure 3: Schematic diagram of repository structure and radionuclide transport considered in the compartment model. Horizontal arrows in the NFR regions represent advective transport of radionuclides by groundwater flow. Horizontal arrows become darker in the downstream compartments, simulating concentration increase. Vertical arrows in the buffer regions represent the radionuclide transport by diffusion.

Table 1: Assumed Parameters for Radionuclides and the Repository.

	Description and Values	
λ	^{237}Np decay constant.	3.2×10^{-7} yr^{-1}
K	Np retardation factor in the buffer region.	4900 †
R	Np retardation factor in the NFR region.	2600 †
C^*	Np solubility in the groundwater.	2.0×10^{-5} mol/m^3 †
M_0	Initial mass of ^{237}Np in a single waste matrix.	3.7 mol †
D	Diffusion coefficient in the buffer.	0.03 m^2/yr §
F	Volumetric flow rate of groundwater through the interface between two adjacent compartments in a row.	0.475 m^3/yr ¶
ε	Porosity in the buffer region.	0.3 ‡
ε_p	Porosity in the NFR region.	0.5 ‡
V	Volume of the NFR region in a compartment.	9.1 m^3 ‡
v	Pore velocity of groundwater.	1 m/yr ‡
S	Surface area of the waste matrix.	1.8 m^2 ‡
A	Cross-sectional area of a compartment.	0.9 m^2 ‡
L	Thickness of the buffer region.	0.98 m ‡

† Ref. [7], § Ref. [9], ‡ Ref. [10], ¶ $F = \varepsilon_p A v$.

In the waste matrix region, the mass of a radionuclide changes due to radioactive decay and its release into the buffer region. The release rate of a radionuclide into the buffer is determined by selecting the constant matrix dissolution rate or the solubility-limited diffusive mass flux at the waste-matrix/buffer interface, whichever is smaller.

In the buffer region, transient molecular diffusion of the radionuclide is treated in one-dimensional slab geometry with inclusion of radioactive decay. The buffer is assumed to be homogeneously porous. There is no advection in the buffer.

Uncontaminated water enters the NFR of the first compartment in the row. The water in the pores of the NFR is contaminated by radionuclides released from the waste matrix and its transport through the buffer by diffusion. Contaminated water in the NFR continues to flow into the NFR of the second compartment in the row, and contacts with the buffer there. This water gets additionally contaminated by radionuclides released from the second canister. In this fashion, the groundwater flowing in the row through the NFR is assumed to be increasingly contaminated before it finally flows out of the repository from the NFR of the N-th compartment.

The concentration gradient in the buffer is the largest in the first compartment, resulting in the largest mass flux from the buffer. While decrease in radionuclide mass in the waste matrix occurs for all compartments, the complete depletion of radionuclide from the waste matrix occurs at the earliest time in the first compartment in the row. Then, the second compartment is exposed to the highest mass flux among the remaining ones. In this fashion, the radionuclide mass depletes from the upstream compartment to the downstream end of the row.

The radionuclide concentration in the NFR region of the n-th compartment from the upstream side of the row is determined by its radioactive decay, advective mass flux from the adjacent upstream compartment (n–1), advective mass flux leaving the compartment n, and diffusion from the buffer into the NFR. The concentration is assumed to be uniform in the NFR region of a compartment, but varying with position n. The mass balance equation in the NFR region is written as

$$\varepsilon_p RV \frac{dC_n}{dt} = -\lambda \varepsilon_p RVC_n + FC_{n-1} - FC_n + Q_n(C_n,t) \ , t>0, \ n=1,2,\ldots,N \ , \ C_0 \equiv 0, \qquad (2)$$

where $C_n(t)$ [mol/m^3] is the concentration of a radionuclide in pore water in the NFR region of the n-th compartment at time t [yr], and $Q_n(C_n,t)$ [mol/yr] is the mass release rate from the buffer. The release rate Q_n is assumed to be proportional to the concentration gradient at buffer/rock interface, and hence depends on C_n. Volumetric flow rate, F, of groundwater is defined as $F = \varepsilon_p A v$, where A is the cross-sectional area of the NFR region in a compartment, and v is the pore velocity of the groundwater. The water flowing into the first compartment is uncontaminated ($C_0 \equiv 0$). Definitions of the parameters are given in Table 1. F, ε_p, R, and V are assumed to be constant in time and space.

The difference between the independent single-canister model (Figure 1) represented by Eq. (1) and the present model represented by Eq. (2) can be considered as follows. In the independent single-canister model, $n = N = 1$, and the mass release rate, Q, is obtained by assuming that the concentration in the NFR is zero [3,5,6,7]. In the notation of Eq. (2), $Q = Q_1(0,t)$. To assume the zero concentration at the interface between the EBS and the NFR, it should be assumed that the water flow rate, F, through the NFR is infinitely large. If the radionuclide released from the EBS into the NFR is assumed to be instantaneously swept by an infinitely large water flow F in the NFR, maintaining C_1 at zero for all time, the term in the left side and the first term in right side in Eq. (2) are dropped. The second term in the right side of Eq. (2) is zero for $n = 1$ by definition. Then, provided that FC_1 is finite and non zero, Eq. (2) is reduced to $0 = -FC_1 + Q_1(0,t)$, which is formally equivalent to Eq. (1). This comparison shows that determination of the flow rate, F, in the previous models is arbitrary and

inconsistent, because of the following reason. C_1 must be non-zero in order to have a non-zero far-field concentration. $Q_1(0,t)$ is finite and non-zero. But, because F is assumed to be infinitely large, C_1 becomes zero.

The radionuclide mass in the far field is determined by the rate of release, FC_N, from the NFR region of the N-th compartment in the repository, and by radioactive decay. Since the concentration C_N is affected by C_{N-1}, which is affected by C_{N-2}, and so forth, the mass in the far field is also affected by the interactions among the compartments in the repository.

The mathematical model is described in a more detailed manner elsewhere [9]. Computer code, "VR," [11] has been developed for the present model. Numerical results have been obtained by this code in this study.

4- RESULTS AND DISCUSSIONS

4.1 Effects of Configuration

The radionuclide transport in Configuration (2) is investigated with ^{237}Np. The data for the radionuclide and for the repository are shown in Table 1. Mass of ^{237}Np in each region of the compartment has been obtained in detailed calculations, and is plotted as a function of time in Figure 4. The mass has been normalized with the mass of the radionuclide in the waste matrix, M_0, at the beginning of the release (t=0). We refer M_0 as the initial mass hereafter. The mass in the NFR has been calculated from $C_1 R \varepsilon_p V$. The same results as shown in Figure 4 apply for any number, N, of compartments in this configuration (2).

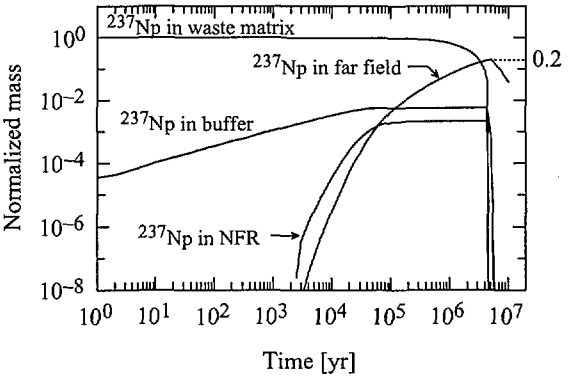

Figure 4: Mass of ^{237}Np in Configuration (2), normalized by the initial mass, M_0, in the waste matrix.

The normalized mass in the buffer increases immediately after t = 0 when ^{237}Np release from the waste matrix starts. ^{237}Np, having a sufficiently long half-life to survive its diffusion time in the buffer, reaches the outer boundary of the buffer after 2000 years, and starts being released into the NFR. At the same time, mass release into the far field starts (Figure 4). Release into the far field continues until it completely depletes in the waste at 5.5 × 10^6 yr when a rapid drop in the normalized masses in the waste matrix is observed. After this rapid drop, ^{237}Np exists only in the far field, whose mass decreases exponentially by radioactive decay. The maximum mass of ^{237}Np in the far field at 5.5 × 10^6 yr is observed to be 20% of the initial mass.

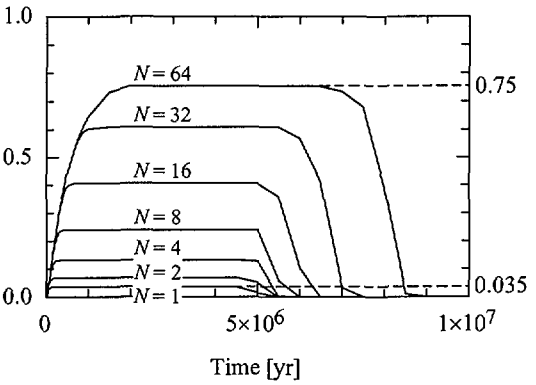

Figure 5: Concentration of ^{237}Np, normalized by the solubility C of Np, in the groundwater leaving the repository for N compartmenst. Configuration (2) corresponds to the case with N=1, whereas configuration (1) corresponds to the cases with N = 2, 4, ..., 64*

The transport of ^{237}Np is calculated with the VR code for Configuration (1) in length with N = 2, 4, 8, 16, 32, and 64, and compared with Configuration (2). In Figure 5, the normalized concentration of ^{237}Np, C_N/C^*, in the groundwater leaving the last (N-th) compartment of the row is plotted as a function of time for different values of N. Here, C^* is the solubility of Np in the groundwater.

For all configurations, the concentration increases at early times until it reaches a steady-state plateau. The plateau concentration is maintained until the complete depletion in the waste matrix occurs in one compartment after another starting at the upstream side of the row. For a greater N, the complete depletion in the waste matrix in the N-th compartment occurs at a later time, and hence the steady-state plateau lasts longer.

It is observed from Figure 5 that the plateau concentration increases as N increases. It is also seen that the plateau concentration does not increase proportionally with N if the initial inventory (NM_0) of ^{237}Np in the row of N compartments is N times greater than that (M_0) of the single-compartment configuration. For example, the plateau concentration of the 64-compartment configuration (0.75 in Figure 5) is less than 64 times that of the single-compartment configuration (0.035 in Figure 5).

The steady-state concentration, C_N^{SS} [mol/m^3], in the groundwater leaving the last compartment of the row is obtained analytically by setting the time derivative term in (2) to be zero. Assuming steady-state diffusion in the buffer regions and that the concentration at the waste-matrix/buffer interface is constant at C^*, C_N^{SS}/C^* is ob-

tained as

$$C_N^{SS}/C^* = Gf(N;\gamma)\ ,\ N = 1,2,..., \tag{3}$$

where

$$G \equiv \frac{\beta}{\lambda R \varepsilon_p V + F + \beta \cosh \alpha L}\ ,\ f(N;\gamma) \equiv \frac{1-\gamma^N}{1-\gamma}\ , \tag{4}$$

$$\alpha \equiv \sqrt{\frac{K\lambda}{D}}\ ,\ \beta \equiv \frac{S\varepsilon D\alpha}{\sinh \alpha L}\ ,\ \gamma \equiv \frac{F}{\lambda R \varepsilon_p V + F + \beta \cosh \alpha L}\ ,\ \lambda > 0\ .$$

The parameter values shown in Table 1 give the values $G = 0.035$ and $\gamma = 0.96$. In case of $N = 1$, the function $f(N=1;\gamma)$ in (3) becomes unity, and the normalized steady-state concentration is obtained as 0.035. This steady-state concentration is in good agreement with the numerical results obtained by the VR code shown in Figure 5.

The parameter G defined in (4) is physically interpreted as the concentration reduction by diffusion in the EBS and advection in the NFR in a single compartment. The function $f(N;\gamma)$ defined in (4) represents the effect of radionuclide accumulation in the NFR due to multiple compartments. From the analytical expression (4) for $f(N;\gamma)$, the steady-state concentration C_N^{SS} does not increase proportionally with N. It can be readily shown that $C_N^{SS}/N < C_1^{SS}$ for $N = 2,3,....$ This is also confirmed by the numerical results obtained by the VR code shown in Figure 5. As N tends to infinity, C_N^{SS}/C^* approaches a limit, independent of N,

$$\lim_{N\to\infty} C_N^{SS}/C^* = Gf_\infty(\gamma) \text{ where } f_\infty(\gamma) \equiv 1/(1-\gamma)\ ,\ \text{if}\ \gamma < 1. \tag{5}$$

$Gf_\infty(\gamma)$ is calculated as 0.80 for the parameter values shown in Table 1.

These effects of the canister multiplicity have not been observed in previous performance assessments, which are based on the independent single-canister model.

4.2 Effects of Mass Reduction

Effects of mass reduction on the concentration entering the far field are investigated by decreasing radionuclide mass in each canister by the same factor. The number of canisters is kept unchanged ($N = 64$) hereafter. In the "no mass reduction" case, the initial mass placed in the row is $3.7 \times 64 = 237$ mol. For the "1/10 mass reduction" case, the initial mass placed in the row in 64 canisters is 23.7 mol. The 1/100 and 1/1000 reduction cases are defined similarly.

In Figure 6, the change of the concentration $C_1(t)$ as a function of time is shown for the *perpendicular-to-flow* configuration (i.e., Configuration (2) in Figure 2). For the cases with no, 1/10-, and 1/100-reduction, the magnitude of the concentration is on the same order. The concentration time span decreases as the mass is reduced, because the release from the waste matrix is limited by the solubility of neptunium. In the 1/1000-reduction case, the concentration is substantially smaller than the other three cases. This is because the release from the waste matrix is controlled by the waste-matrix dissolution. The rate of mass release into the far field is given by $64FC_1(t)$.

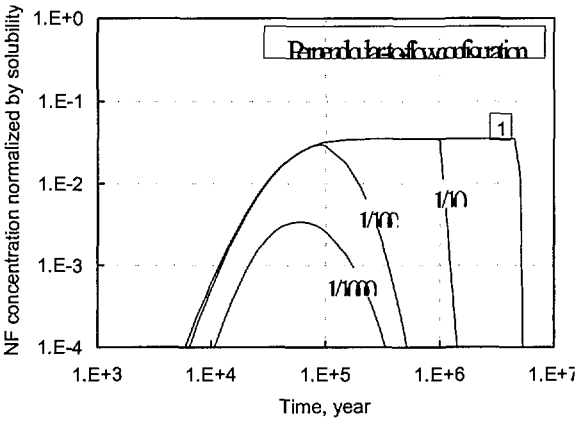

Figure 6: Effect of initial ^{237}Np mass reduction on ^{237}Np concentration $C_1(t)$ in the water leaving the repository for the perpendicular-to-flow configuration. The fractions indicate the mass reduction.

This result confirms the comments made in the legend of Figure 1. The concentration depicted in Figure 6 is the inlet boundary condition for the far-field model. Because the order of the magnitude of the peak inlet boundary concentration is not changed for 1, 1/10, and 1/100 reduction cases, the far-field concentration would not differ by reducing the radionuclide mass in the waste with the perpendicular configuration.

In Figure 7, the change of the concentration $C_{64}(t)$ as a function of time is shown for the *parallel-to-flow* configuration (i.e., Configuration (1) in Figure 2). The rate of mass release into the far field is given by $FC_{64}(t)$. Due to accumulation during the transport through 64 compartments, the concentration $C_{64}(t)$ is close to the solubility for the mass reduction of 1 and 1/10.

With the parallel-to-flow configuration, $C_{64}(t)$ decreases clearly by the mass reduction. Therefore, with

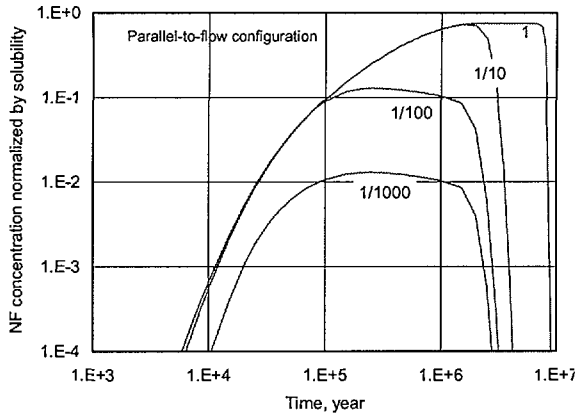

Figure 7: Effect of initial ^{237}Np mass reduction on ^{237}Np concentration $C_{64}(t)$ in the water leaving the repository for the parallel-to-flow configuration.

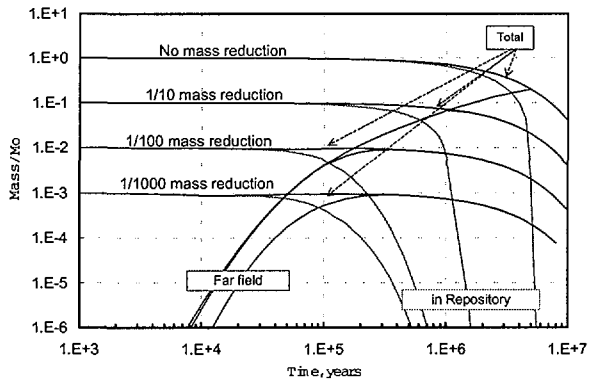

Figure 8: Effect of initial ^{237}Np mass reduction on mass distribution in the repository and in the far field for the perpendicular-to-flow configuration.

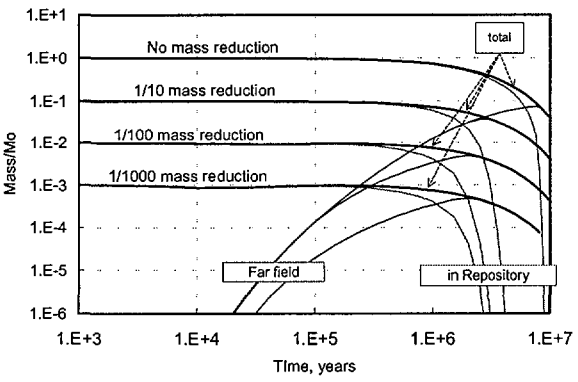

Figure 9: Effect of initial ^{237}Np mass reduction on mass distribution in the repository and in the far field for the parallel-to-flow configuration.

$C_{64}(t)$ as the inlet boundary condition for the far-field analysis, effects of P-T scheme could be expressed more sensitively than with $C_1(t)$. Also, it is observed that the concentrations $C_1(t)$ for the perpendi-cular-to-flow configuration is smaller than $C_{64}(t)$ for the parallel-to-flow configuration. It implies that the previous models *under*estimate the inlet boundary concentration for the far-field analysis.

Figure 8 shows the temporal change of the mass of ^{237}Np in the row of 64 compartments and of the mass in the far field, for the *perpendicular-to-flow* configuration (2) for four different initial masses. For each case, three curves are shown: the mass in the repository region, the mass in the far-field region, and the total mass. Masses are normalized with 237 mol.

For no mass reduction case, the mass in the far field increases with time, while the mass in the repository decreases rapidly after 1 million years, and tends to zero at 5.5 million years. This case is the same as that depicted in Figure 4. The far-field-mass curve coincides with the total-mass curve at that time. Most of the initial mass of ^{237}Np remains in the repository until 1 million year. About 4/5 of the initial mass of Np decays in the repository, and 1/5 accumulates in the far field at 5.5 million years.

With mass reduction by a factor of 1/10, 1/100 or 1/1000, the mass in the repository is reduced by the corresponding factor at early times. With a smaller mass in the repository, the mass in the repository becomes zero earlier. Virtually all neptunium initially existing in the repository is released into the far field. However, because the initial mass is reduced, the mass released into the far field is also reduced by the same factor.

For the no-mass-reduction, 1/10-, and 1/100-reduction cases, the far-field-mass curve traces the same trajectory at early times. This is because the release from the waste matrix is limited by the solubility. The far-field-mass curve for the 1/1000 reduction case is located below the other three curves, because the initial mass is reduced to the extent that the release is not limited by the solubility anymore, as is observed in Figure 6.

In Figure 9, same quantities are plotted for the *parallel-to-flow* configuration. Mass released in the upstream compartments accumulates as water flows in the row. Release from EBS in down-stream compartments becomes smaller, so that the release from the repository is smaller than that from the repository in the perpendicular-to-flow configuration. By comparing Figure 9 with Figure 8, the far-field mass in Figure 9 is smaller than that in Figure 8 for the same initial mass. Due to smaller release from the repository (or longer residence time in the repository), more neptunium decays while it is in the repository. Thus, the mass-in-the-repository curves are shifted to the right, compared with those in Figure 8. In either configuration (1) or (2), the radionuclide mass in the repository or in the far field differs by reducing the initial radionuclide mass in the repository.

The evaluated radionuclide concentration in water entering the far field is significantly different, depending on which configuration of multiple canisters is assumed. It is insensitive to mass reduction if evaluated with the perpendicular-to-flow configuration, whereas sensitive if evaluated with the parallel-to-flow configuration. The radionuclide masses in the repository and in the far field are similarly sensitive to the initial mass reduction for both configurations.

5- CONCLUSIONS

A repository model has been developed, where canister multiplicity and their spatial configuration are taken into account. By comparing the previous independent single-canister model with the present model, the following conclusions have been drawn.

- The repository configuration has significant effects on radionuclide release from the repository into the far field, especially for long-lived radionuclides, such as ^{237}Np.
- The insensitivity of the radionuclide concentration to the initial mass reduction has been observed in the perpendicular-to-flow configuration (2), which is the same configuration as applied in previous performance assessment studies [3,5,6,7].
- For the parallel-to-flow configuration (1), the concentration of ^{237}Np released from the repository increases as the number, N, of compartments per row increases. As N tends to infinity, the normalized concentration approaches the value given by Eq. (5) and becomes independent of N.
- For the parallel-to-flow configuration (1), the concentration in the water leaving the repository decreases as the initial mass is reduced. Thus, by taking into account canister arrangement and interaction among multiple canisters in the repository, the mass reduction can actually have significant effects on the repository performance.
- In either configuration (1) or (2), the radionuclide mass in the repository or in the far field is reduced proportionally by the reduction of initial mass. At early times ($<10^5$ yr), due to solubility limit, the effect of the initial mass reduction on the far-field mass is not significant.
- For a compartment row tilted with respect to the water flow direction, the water flow can be decomposed into parallel and perpendicular components, for which the parallel and perpendicular configurations considered in this study can be applied.

ACKNOWLEDGEMENT

The authors are grateful for Mr. D. Kawasaki for his help in numerical calculations.

REFERENCES

[1] Ramspott, L. D., Choi, J.-S., Halsey, W., Pasternak, A., Cotton, T., Burns, J, McCabe, A, Colglazier, W., and Lee, W. W.-L., *Impact of New Developments in Partitioning and Transmutation on the Disposal of High-Level Nuclear Waste in a Mined Geologic Repository*, UCRL ID-109203, Lawrence Livermore National Laboratory (1992).

[2] Pigford, T. H., Actinide Burning and Waste Disposal, MIT International Conference on the Next Generation of Nuclear Power Technology, UCB-NE-4176, Univ. of California, Berkeley (1990).

[3] Ahn, J., Integrated Radionuclide Transport Model for an HLW Repository in Water-Saturated Geologic Formations, *Nuclear Technology*, **121**, 24-39 (1998).

[4] Lowenthal, M. D., Ahn, J., Chambré, P. L., Greenspan, E., Kastenberg, W. E., Park, B., and Stone, N., Impacts of Waste Transmutation on Repository Hazards, *Proc. Global '99, Int. Conf. on Future Nuclear Systems*, Jackson Hole, Wyoming (1999).

[5] US Department of Energy, Viability Assessment of a Repository at Yucca Mountain, DOE/RW-0508 (1998).

[6] Civilian Radioactive Waste Management System Management and Operating Contractor (CRWMS M&O), Total System Performance Assessment-Viability Assessment (TSPA-VA) Analysis Technical Basis Document, Chapter 6: Waste Form Degradation, Radionuclide mobilization, and Transport Through the Engineered Barrier System, TRW Environmental Safety Systems Inc., B00000000-01818-4301-00001 (1998).

[7] Japan Nuclear Cycle Development Institute, *Second Progress Report on Research and Development for the Geological Disposal of HLW in Japan, H12: Project to Establish the Scientific and Technical Basis for HLW Disposal in Japan*, **3**, V (2000).

[8] US Department of Energy, *A Roadmap for Developing Accelerator Transmutation of Waste (ATW) Technology,* A Report to Congress, DOE/RW-0519 (1999).

[9] Ahn, J., Possibility of Safety Improvement for Vitrified HLW Geologic Disposal by Partitioning and Transmutation, *Proc. Global '99, Int. Conf. on Future Nuclear Systems*, Jackson Hole, Wyoming (1999).

[10]Ahn, J., Criticality Safety Assessment for a Conceptual High-Level-Waste Repository in Water-Saturated Geologic Media, *Nucl. Technol.*, **126**, 303 (1999).

[11]Tsujimoto, K., D. Kawasaki, J. Ahn, and P. L. Chambré, *Virtual Repository (VR) Version 1.0 Operation Manual*, Department of Nuclear Engineering, University of California, Berkeley, California (2000).